1st Corrosion and Materials Degradation Web Conference (CMDWC 2021)

Slurry erosion resistance of ferritic X10CrAlSi18 and austenitic AISI 304 stainless steels

Marta Buszko

supervisor: dr hab. inż. Alicja Krella, prof. IMP PAN

Institute of Fluid–Flow Machinery, Polish Academy of Sciences

Correspondence: marta.buszko@imp.gda.pl

Slurry erosion

Surface degradation due to an interaction of solid particles (erodents) suspended in the liquid medium with an eroded surface is called **slurry erosion** [1-3].

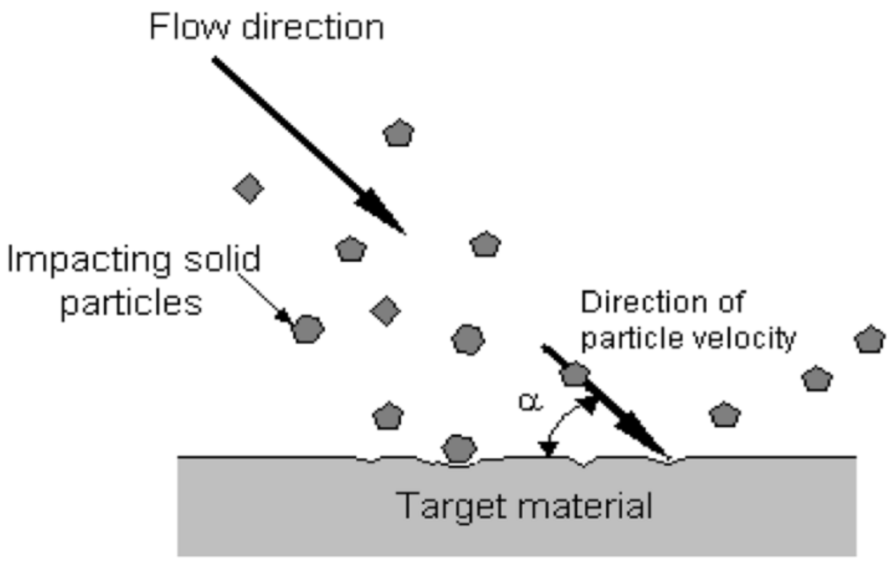

Fig. 1. The scheme of slurry erosion process [3]

Factors affecting slurry erosion [1-3]

Operating Conditions

- impact velocity
- impact angle
- solid particles concentration
- condition of medium (liquid density, chemical activity and temperature)

Properties of Eroding Particle

- size,
- shape,
- hardness

Properties of Target Material

- mechanical and endurance properties like toughness, fatigue, yield strength, ultimate tensile strength, hardness,
- microstructure

Experimental details

Slurry erosion test rig	Materials	Metodology

Slurry erosion test rig

- The slurry pot consists of a cylindrical tank with a capacity of 6.4 L, a mixing system and a drive kit.
- Four baffles were mounted at the inner wall of the slurry pot to minimize centrifugation of the fluid due to the rotation of the propeller. The propeller is mounted to prevent sedimentation of solid particles.
- The samples are placed in two specimen holders, which are designed to rotate from 0° to 90°.

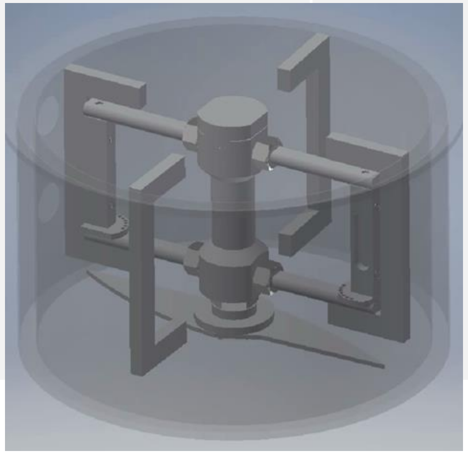

Fig. 2. The scheme of slurry pot tester

Materials

The materials (as-received condition) used in this investigation:

- ✓ ferritic X10CrAlSi18 stainless steel (body-centered cubic)
- ✓ austenitic AISI 304 stainless steel (face-centered cubic)

The solid–liquid mixture was prepared by mixing steel solid particles with a diameter of 520 μm and hardness of 528 HRC with tap water.

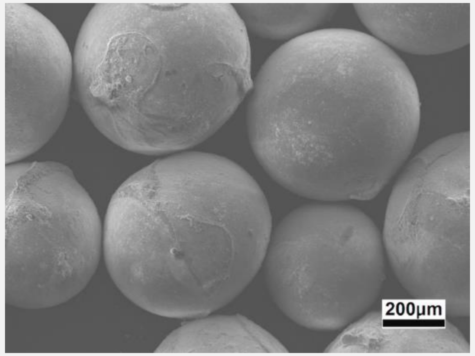

Fig. 3. Solid particles / erodents

Metodology

<u>Erosion test parameters</u>

- rotational speed: 1012 rpm,
- impact angle: 90°,
- concentration of erodents: 12.5%,
- total time of the slurry tests: 600 min.

➢ Before the tests and after each test exposure the test samples were cleaned, dried and reweighed using an analytical balance with a sensitivity of 0.1 mg in order to determine the erosion curves.

➢ The surface microhardness was measured using the INNOVATEST FALCON 401 Vickers Hardness Tester with 500 gf load and dwell time of 10 s. The microhardness measurements were performed up to 240 min of studies and at the end of the tests.

➢ The surface roughness was examined every exposure using the SJ-301 Mitutoyo Surface Roughness Tester.

➢ The microscopic observation after all slurry erosion tests was studied using a scanning electron microscope Hitachi SU3500.

Mass losses / Erosion rate

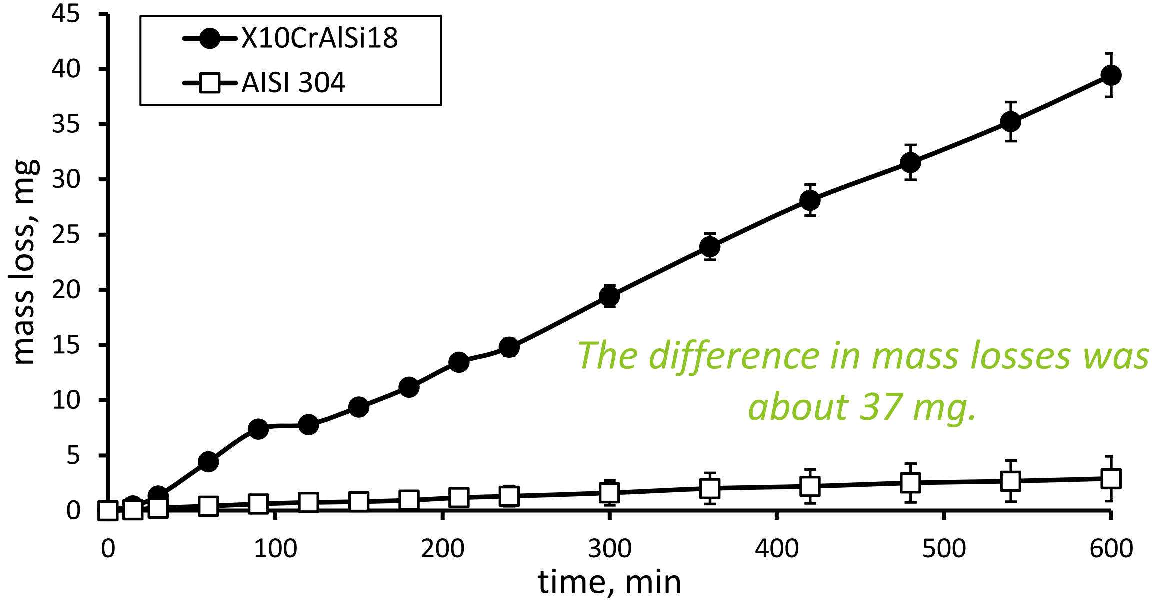

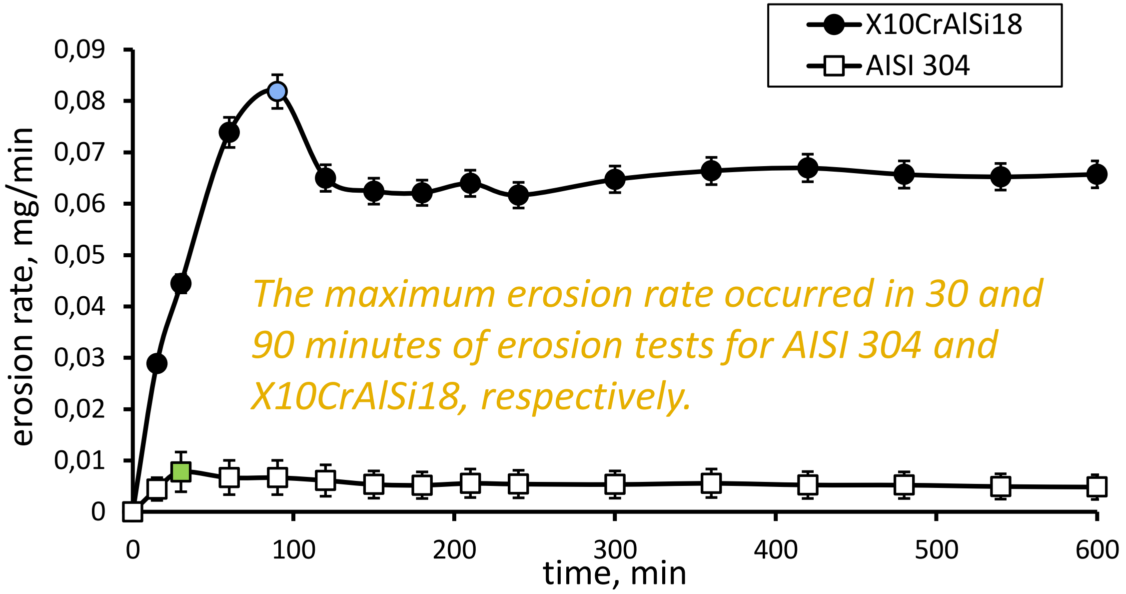

grain size: 47±7 µm

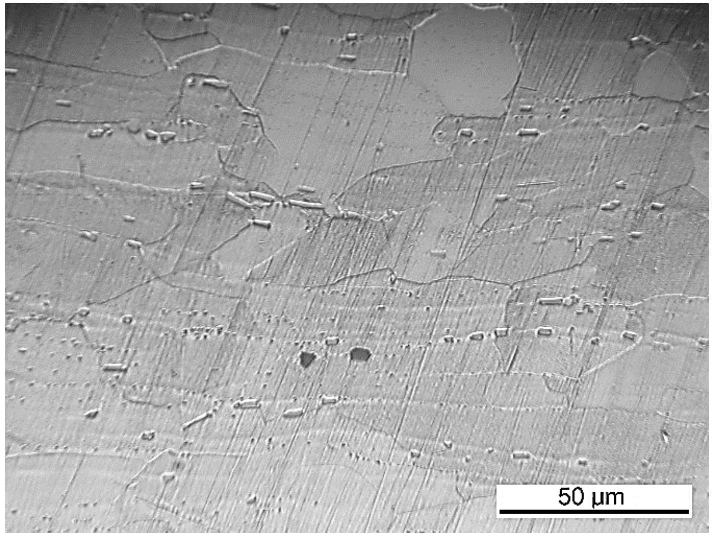

Fig. 4. Microstructure of ferritic X10CrAlSi18 stainless steel

grain size: 16±3 µm

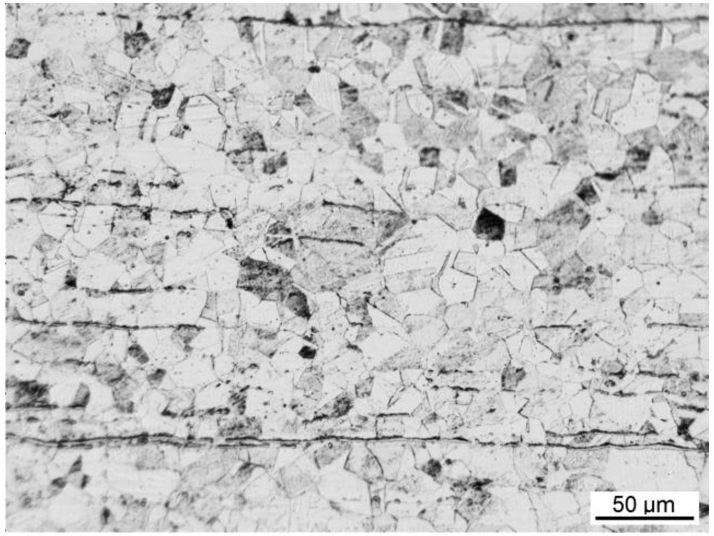

Fig. 5. Microstructure of austenitic AISI 304 stainless steel

Hardness

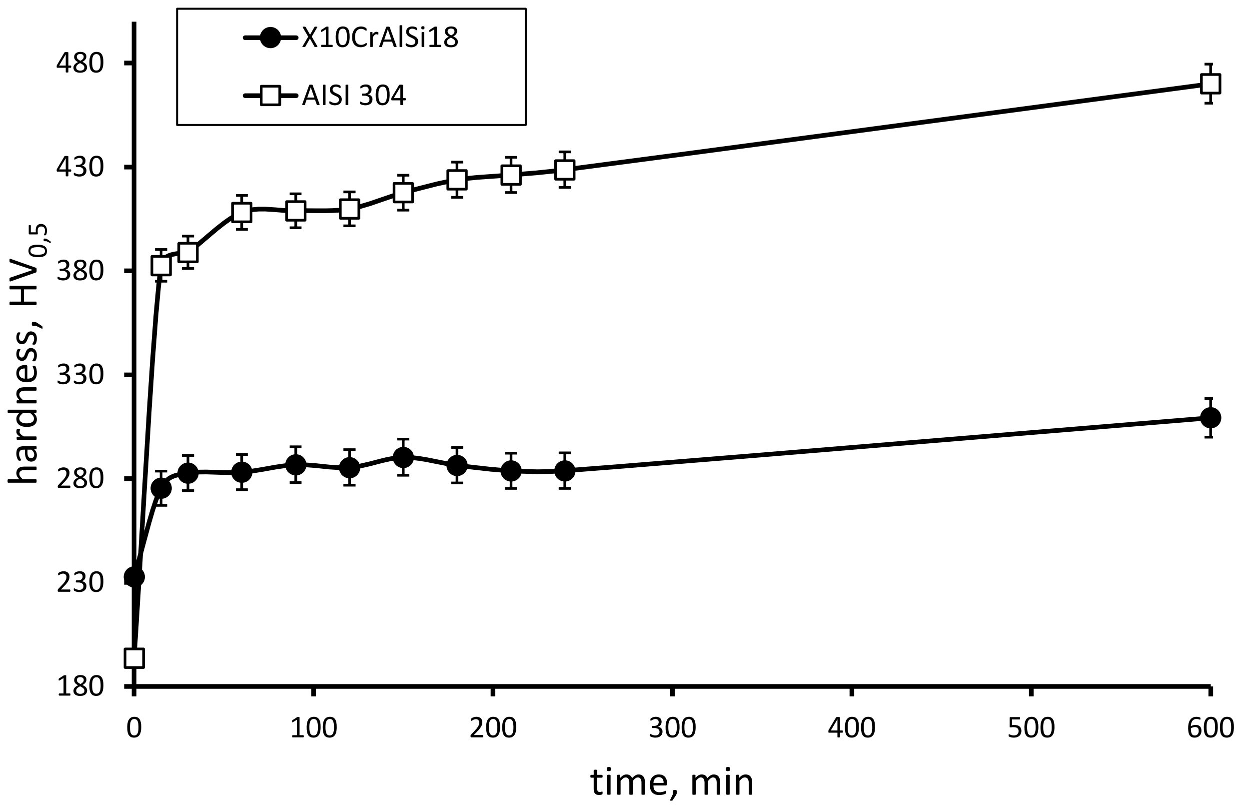

- The exposure of X10CrAlSi18 and AISI 304 steels to slurry erosion caused a significant increase in surface hardness in the initial period of testing.
- The strain hardening effect was about 33% and 143% for ferritic and austenitic steels, respectively.
- The microstructure and the strain hardening of the eroded materials were more important than the initial hardness.
- The hardness after the erosion test of the austenitic steel was higher about 161 HV than the ferritic steel.

Roughness parameter: Ra and Rz

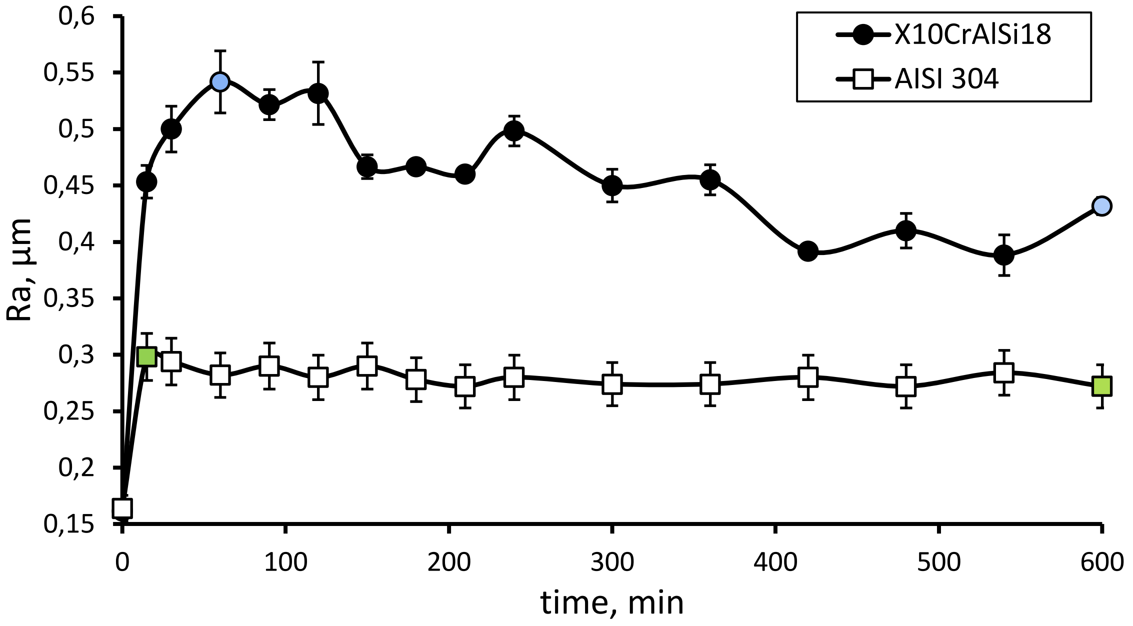

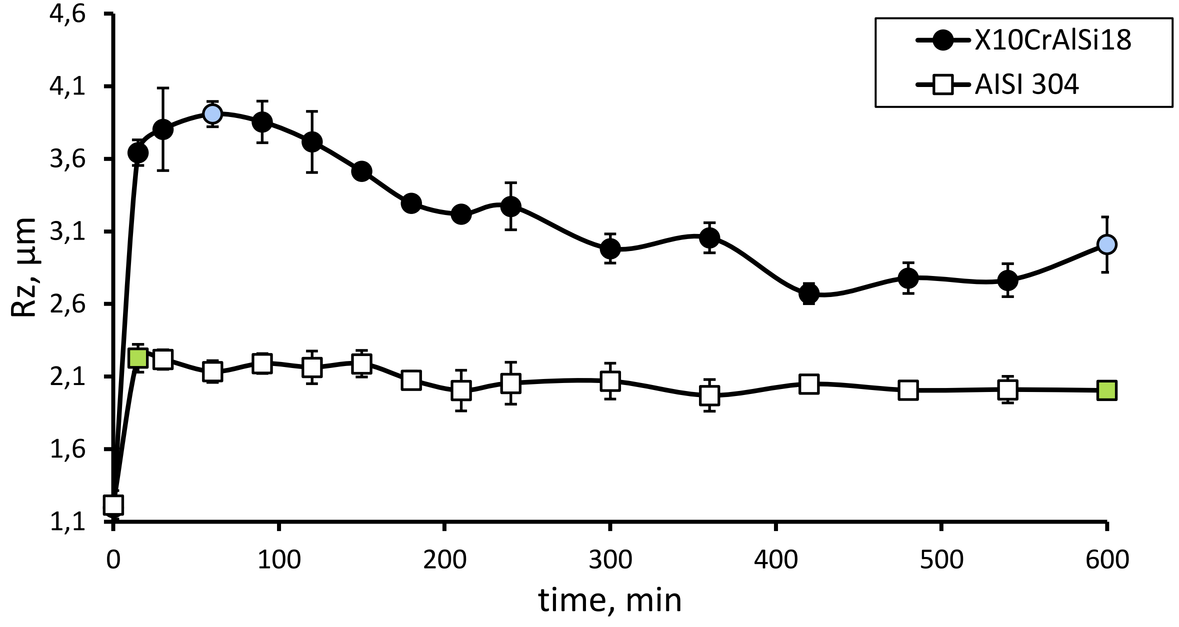

- X10CrAlSi18 steel obtained higher parameters Ra and Rz compared to AISI 304 steel.
- The roughness parameters Ra and Rz of AISI 304 steel, after reaching its maximum value, remained at a similar level throughout the exposure time.
- The values of the Ra and Rz parameters of ferritic steel began to drop significantly after reaching the maximum value.
- The roughness parameters Ra and Rz increased with the decrease in the hardness of the eroded steel.

Microscopic observation

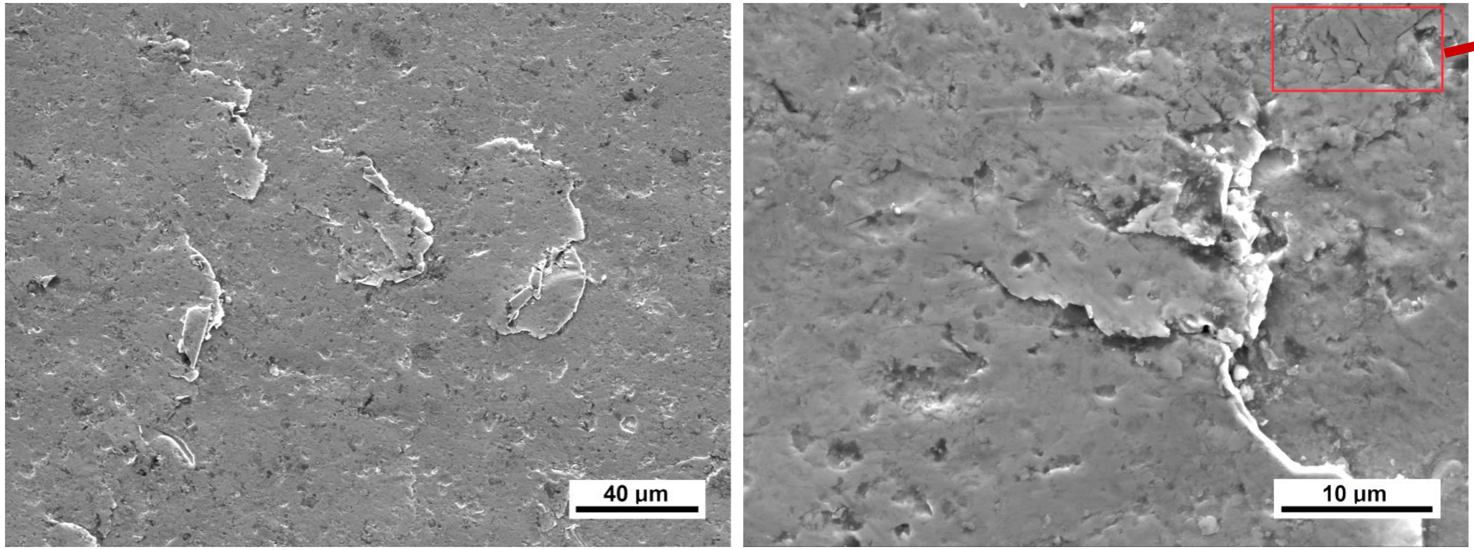

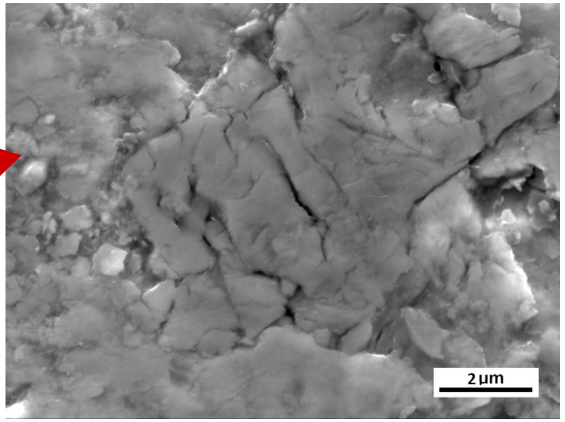

Fig. 6. SEM images of ferritic X10CrAlSi18 steel after the slurry erosion test

- ✓ Craters, cracks and extensive flakes were observed on the surface of ferritic X10CrAlSi18 steel (Fig. 6). The size of craters was in the range from 2 µm to 6 µm.
- ✓ The erosion mechanism was determined by brittle fracture.

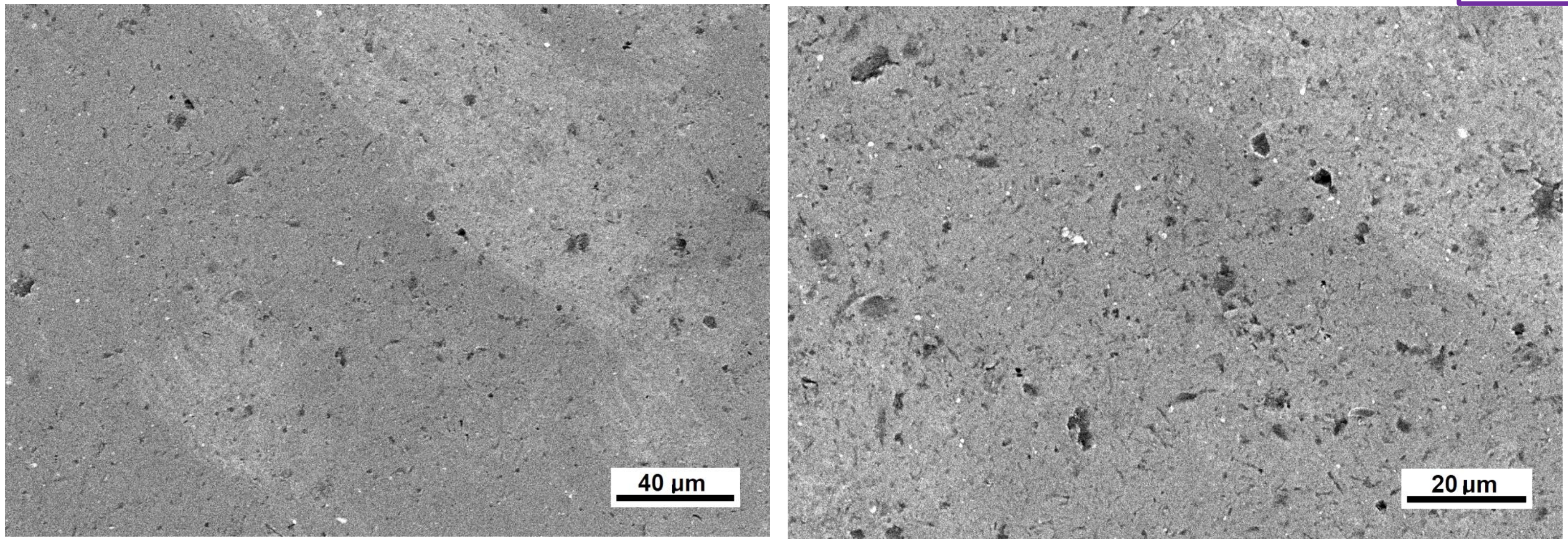

Fig. 7. SEM images of austenitic AISI 304steel after the slurry erosion test

- ✓ Indentations, craters, and slightly wave texture were observed on the surface of austenitic AISI 304 steel (Fig. 7). The size of craters was in the range of 1–4 µm and some of the craters with the size of 6 µm.
- ✓ The erosion mechanism was determined by plastic deformation.

Erosion efficiency parameter, η

Sundararajan et al. [4] defined the erosion efficiency, η, as the ratio of the removed target material volume to the crater volume. The erosion efficiency, η, was calculated according to equation (1).

$$\eta = \frac{2E_v H}{V^2} \cdot 100\% \quad (1)$$

, where:
E_v – erosion rate [m^3/kg]
H – hardness of target material [Pa]
V – impact velocity [m/s]

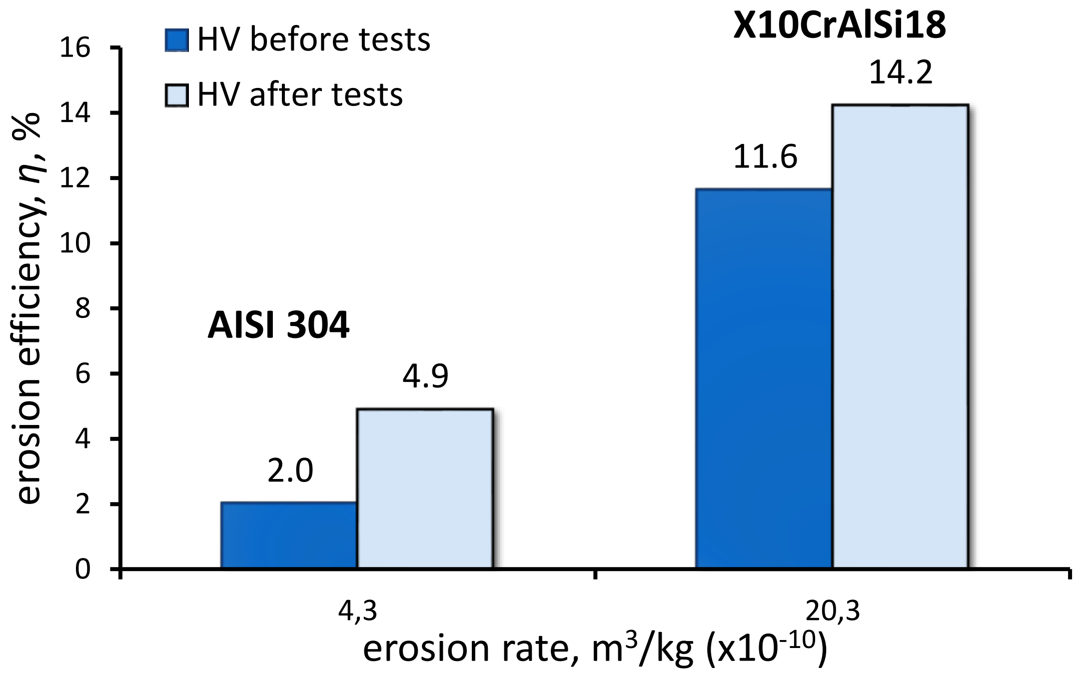

- According to Ref. [4], values of this parameter below about η = 10% indicate a ductile erosion mode, while above about η = 10%, it indicates a brittle mode of erosion.
- The erosion efficiency parameter (1) was η = 2.0% and η = 11.6% for AISI 304 steel as well as X10CrAlSi18 steel, respectively. In addition, the final hardness of the eroded material increased, this also leads to an increase in the erosion efficiency to 4.9% and 14.2%. Thus, according to Ref. [4] ferritic steel is characterized by a brittle erosion mode and austenitic steel by ductile erosion mode.
- These results correlate well with the observation of the microstructure after the erosion test.

Summary

- The results confirm that the microstructure, lattice structure and strain hardening effect on the erosion behavior of eroded steels.
- Ferritic X10CrAlSi18 steel with bcc (body-centered cubic) lattice structure showed lower erosion resistance than this with fcc (face-centered cubic) lattice structure (austenitic AISI 304 steel). The ferritic steel with a bcc lattice structure had higher mass losses than could be expected from their hardness. The mass losses of X10CrAlSi18 steel were 93% higher compared to the AISI 304 steel.
- Hardness increased with increasing exposure time. In the first 15 minutes of erosion tests, the increase in hardness was 18% and 88% for ferritic and austenitic steels, respectively. The strain hardening effect was about 33% and 143% for ferritic and austenitic steels, respectively.
- As the erosion rate increased, the roughness parameters Ra and Rz increased. X10CrAlSi18 steel obtained higher Ra and Rz compared to AISI 304 steel. In the first 15 minutes of erosion tests, the increase in roughness parameter Ra (Rz) was about 182% (203%) and 88% (83%) for ferritic and austenitic steels, respectively.
- The erosion mechanisms for ferritic steel involve brittle fracture, while austenitic steel was characterized by plastic deformation.
- The erosion efficiency parameter, η, increased with the increase of erosion rate and correlated well with the results obtained from the scanning electron microscope.

Literature

[1] M. H. Buszko and A. K. Krella: *An Influence of Factors of Flow Condition, Particle and Material Properties on Slurry Erosion Resistance*, *Adv. Mater. Sci., vol. 19, no. 2, pp. 28–53, 2019.*

[2] V. Javaheri, D. Porter, and V. T. Kuokkala: *Slurry erosion of steel – Review of tests, mechanisms and materials*, *Wear, vol. 408–409, no. August, pp. 248–273, 2018.*

[3] P. P. Shitole, S. H. Gawande, G. R. Desale, and B. D. Nandre: *Effect of Impacting Particle Kinetic Energy on Slurry Erosion Wear*, *J. Bio- Tribo-Corrosion, vol. 1, no. 29, pp. 1–9, 2015.*

[4] G. Sundararajan and P. G. Shewmon, *A new model for the erosion of metals at normal incidence*, *Wear, vol. 84, no. 2, pp. 237–258, 1983*